

d^0 - d half-Heusler alloys: A class of future spintronic materials

S. Davatolhagh* and A. Dehghan

Department of Physics, College of Sciences, Shiraz University, Shiraz 71946, Iran

(Dated: February 28, 2017)

It is shown by rigorous *ab initio* calculations that half-Heusler alloys of transition metals and d^0 metals, defined by the valence electronic configuration $ns^{1,2}, (n-1)d^0$, can produce all kinds of half-metallic behavior including the elusive Dirac half-semimetallicity that is reported for the first time in the real 3D material CoKSb. Together with the predicted magnetic and chemical stability, this paves the way for massless and dissipationless spintronics of the future. Furthermore, the introduction of d^0 atoms is shown to stabilize the otherwise instable chemical structure of zinc-blende transition metal pnictides and chalcogenides without altering the p - d exchange that is mainly responsible for their half-metallicity, therefore, making their application in spintronic devices feasible.

PACS numbers:

The half-metallic (HM) materials with characteristic 100% spin polarization at the Fermi level, have been regarded as the ideal materials for spintronics due to their potential application as the source of spin-polarized current [1, 2]. Following the seminal work of de Groot et al. [3], predicting for the first time the HM property in half-Heusler (HH) alloy NiMnSb, much work has been devoted to finding other HM materials of Heusler family [4], transition metal (TM) oxides [5], and binary compounds such as zinc-blende TM pnictides or chalcogenides [6–8], and non-TM-based sp -electron HM ferromagnets [9, 10]. More recently, spin gapless semiconductor (SGS) is introduced as another class of HM materials characterized by an open semiconductor band gap for one spin direction, and nearly closed gap for the other [11]. The SGS materials predicted or fabricated so far are mainly the TM-based full-Heusler and inverse full-Heusler compounds with nearly zero but indirect band gaps [12–15]. To the best of our knowledge, there has been no report of SGS in stoichiometric half-Heusler compounds (see, also, Ref. [15]). A particularly interesting kind of SGS that has been shown to exist in a model 2D ferrimagnetic system [16], is the Dirac half-semimetal (DHS), also referred to as Dirac SGS, with its characteristic Dirac node linear dispersion for one spin channel—as in graphene [17]—and an open semiconductor band gap for the other. The experimental realization of DHS materials is envisioned to pave the way for development of ultra-fast and power-efficient spintronics of the future [18]. Although there have been a number of theoretical proposals for the realization of quasi-2D DHS materials [19–27], the complexity of the structures and/or low magnetic transition temperatures, have rendered their fabrication and possible device application a formidable challenge [18]. It is therefore important to find stoichiometric DHS compounds characterized by thermal and magnetic stability at room temperature. To this end, we present, among others, the d^0 - d Dirac half-semimetal HH-CoKSb.

The spin degeneracy of electronic bands in solid state, $E_n(\mathbf{k}, \uparrow) = E_n(\mathbf{k}, \downarrow)$, originates from the simultaneous effect of time-reversal and spatial-inversion symmetry. As pointed out by de Groot et al. [3], the lack of spatial-inversion symmetry in the HH structure in addition to the broken time-reversal symmetry as in ordinary ferromagnets, further removes the spin degeneracy of electronic bands, thus resulting in robust half-metallicity. This makes the HH $C1_b$ structure, space group $F43m$ (No. 216), particularly interesting from both theoretical and technological point of view [28–31]. More explicitly, the crystal structure of ternary HH compounds, such as NiMnSb, consists of fcc Bravais lattice with three atom basis situated on the cube diagonal: main-group sp atom at (0,0,0), high-valent TM1 atom at (1/4,1/4,1/4), and low-valent TM2 atom at (1/2,1/2,1/2) in Wyckoff coordinates. In the d^0 - d HH alloys, introduced in this letter, the low-valent TM2 atom is replaced by a d^0 atom of alkali or alkaline-earth metals defined by the valence electronic configuration $ns^{1,2}, (n-1)d^0$ such that the d^0 atom and the TM atom are first neighbors, whereas the d^0 atom and the sp atom are second neighbors, separated by the TM atom. This arrangement is found to be the energetically most favorable. Despite the intuitive chemical bond view that atoms devoid of d electrons are unable to form d - d covalent bonds [32], it is shown by rigorous density functional electronic structure calculations that d - d bond formation is indeed possible between the d^0 atoms, as defined above, and the TM atoms. Because the empty $(n-1)d$ orbitals of d^0 atom are only about an electron-volt higher in energy than the occupied $ns^{1,2}$, the promotion of electrons to the empty $(n-1)d$ orbitals costs a small amount of energy, which is more than regained or overcompensated by the covalent bonding with neighboring tetrahedrally coordinated TM atoms. This provides the covalent d - d hybrids that stabilize the HH structure, and the double exchange that is mainly responsible for their magnetism and half-metallicity, as in the prototype d^0 - d half-metallic system HH-MnSrP (see, also, Fig. 1 and Fig. 2).

In this letter, the band structure results, the chemical stability tests, and magnetic transition temperatures T_c

*Corresponding Author: davatolhagh@shirazu.ac.ir

are reported for the prototype d^0 - d HH alloys. It is a matter of considerable interest to find that HH-CoKSb exhibits Dirac half-semimetallicity, a property that is being reported for the first time in real 3D materials. This finding paves the way for ultra-fast and power-efficient spintronics of the future. Furthermore, by considering HH-CrKSb, it is shown that the introduction of d^0 atoms stabilizes the otherwise instable chemical structure of half-metallic zinc-blende TM pnictides—in this case CrSb—thus making their application in spintronic devices feasible. The electronic structure calculations are performed on the basis of spin-polarized density functional theory within the framework of self-consistent field plane wave pseudo-potential method as implemented by the PWscf code in Quantum Espresso [33]. The generalized gradient approximation with ultra-soft pseudo-potentials in the scheme of PBE were used [34]. A dense $18 \times 18 \times 18$ k -mesh was employed for Brillouin zone integration. The high kinetic energy cut-offs of 60 Ry and 600 Ry were applied to the plane wave expansion of wave functions and the Fourier expansion of charge density, respectively. Self-consistency is considered to be achieved when the total energy converges to better than 10^{-6} Ry/f.u. (Ry-berg per formula unit).

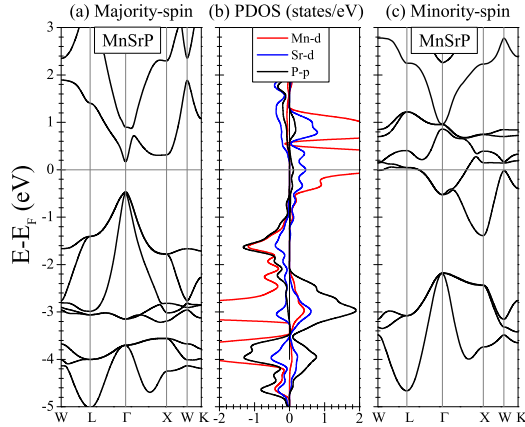


FIG. 1: Spin-resolved band structure and partial density of states of HH-MnSrP.

Figure 1 shows the band structure of HH-MnSrP for both majority- and minority-spin direction. Unlike the usual half-metallic HH compounds such as NiMnSb, in HH-MnSrP the majority-spin electrons are semiconducting while the minority-spin electrons are metallic. The minimum energy for spin excitation or the half-metallic gap is $E_{\text{HM}} = 0.18$ eV, resulting in 100% spin-polarization of conduction electrons, i.e. half-metallicity. The spin-resolved site and orbital projected density of states (PDOS) shown in Fig. 1 (b), indicate that the HM property arises mainly from the exchange splitting of the d bands of TM atom Mn and d^0 atom Sr near the Fermi level. The usual half-metallic HH compounds

such as NiMnSb with more than 18 valence electrons in total, follow the Slater-Pauling relation $M_{\text{tot}} = Z_{\text{tot}} - 18$ [35], where Z_{tot} is the total number of valence electrons per formula unit and M_{tot} is the total magnetic moment in units of Bohr magneton. The Slater-Pauling relations are generally obtained by considering the covalent hybridization of orbitals on neighboring sites [32, 35]. For d^0 - d HH-MnSrP, with $Z_{\text{tot}} < 18$, similar considerations give a Slater-Pauling relation $M_{\text{tot}} = 18 - Z_{\text{tot}}$. The total magnetic moment per formula unit is found to be $M_{\text{tot}} = 4.00$ for MnSrP that is consistent with the above Slater-Pauling relation. The atomic magnetic moments are $M_{\text{Mn}} = 3.98$, $M_{\text{Sr}} = 0.06$, and $M_{\text{P}} = -0.04$. The bulk of magnetic moment is carried by the TM atom Mn. Among the different magnetic structures, the ferromagnetic coupling within fcc sublattice of Mn atoms is found to be the magnetic ground state. The difference between non-magnetic and ferromagnetic total energy is $\Delta E_{\text{NM-FM}} = 1.7$ eV/f.u. On inserting this into the classical Heisenberg spin-Hamiltonian [36], the nearest-neighbor exchange coupling is obtained to be $J = \Delta E_{\text{NM-FM}} / (12M_{\text{Mn}}^2) = 8.85$ meV. By Monte Carlo simulation of the nearest-neighbor Ising model on the fcc sublattice of Mn atoms, the Curie temperature of HH-MnSrP is obtained to be $T_c = 820$ K that is well above the room temperature [37].

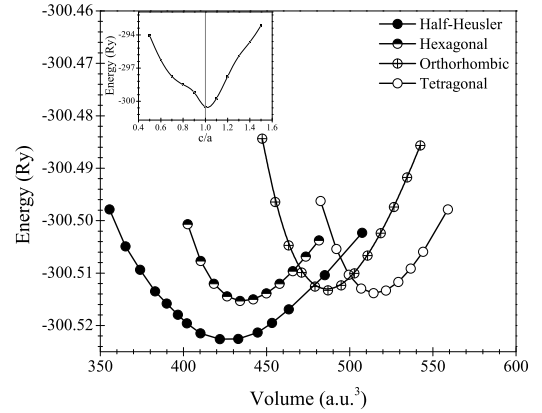


FIG. 2: The total energy vs. volume curves for MnSrP in four different competing structures. Data points are fitted by the Murnaghan equation of state. The inset shows the total energy vs. tetragonalization parameter c/a for HH-MnSrP (the line is guide to the eye).

The rival structures of cubic half-Heusler in which the ternary intermetallic alloys can be realized are the hexagonal Ni_2In , orthorhombic TiNiSi , and tetragonal Fe_2As structure [38]. The stability of HH-MnSrP is checked against the rival structures by calculating the total energy of MnSrP in all the above structures. As it is shown in Fig. 2, half-Heusler is the ground state structure of MnSrP. Also in the inset of Fig. 2, the stability of HH-

MnSrP is tested with respect to constant-volume tetragonalization. There is a global minimum at $c/a = 1$, indicating that the cubic HH-MnSrP is stable with respect to tetragonalization. Furthermore, the formation energy $\Delta H_f = E_{\text{MnSrP}} - (E_{\text{Mn}} + E_{\text{Sr}} + E_{\text{P}})$ of the HH-MnSrP is calculated to check the stability of material against phase separation. The negative value $\Delta H_f = -0.92 \text{ eV}$ indicates that the formation of HH-MnSrP is favored by the constituent elements. All of the above indicate that the HH structure is the thermodynamic ground state of MnSrP. The same stability conclusions obtained for the prototype half-metallic system HH-MnSrP, also are found to apply to the other prototype systems discussed next.

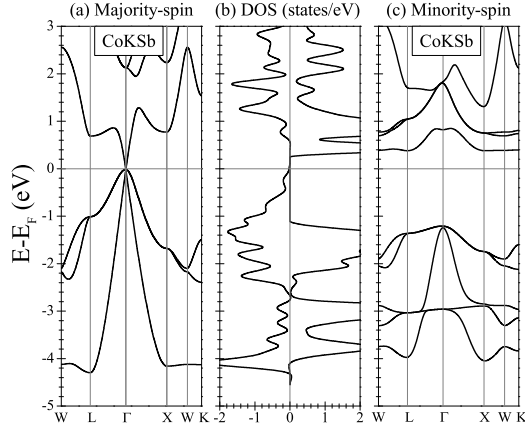


FIG. 3: Spin-resolved band structure and total density of states of HH-CoKSb.

A model system that exhibits Dirac half-semimetallicity consists of itinerant conduction electrons magnetically coupled by a Kondo-type Hamiltonian to a three-sublattice up-up-down ferrimagnet defined on triangular lattice [16]. For a given Fermi level or concentration of conduction electrons, the model system exhibits Dirac nodes in the band structure with 100% spin polarization, thus suggesting the possibility of the realization of Dirac half-semimetals in realistic transition metal and rare-earth compounds [16]. Here, we report for the first time the DHS property in the real 3D stoichiometric material HH-CoKSb. Figure 3 shows the band structure of HH-CoKSb. There is a sizable gap in the minority-spin band structure and the Fermi level falls within the gap. In the majority-spin channel, however, the conduction and the valence bands touch directly at the Γ point and the Fermi level. The linear dispersion of the conduction band and one of the valence bands in majority-spin channel, indicates that both carriers (electrons and holes) have vanishingly small band-mass, high mobilities, and both are 100% spin-polarized. However, because there are three valence bands touching the conduction band at the Fermi level, two of which have ordinary parabolic dispersion, there

will be both massive and massless holes in the majority-spin channel at finite temperature. The Fermi velocity of Dirac fermions is found to be $v_F = 8.4 \times 10^5 \text{ m/s}$ that is 84% of that in graphene [17]. CoKSb shows the highest Fermi velocity compared to the quasi-2D DHS materials that have been theoretically predicted so far [19, 21, 23, 24, 27].

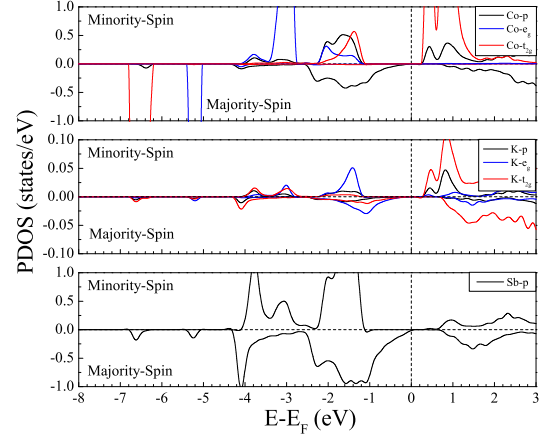


FIG. 4: Spin-resolved site and orbital projected density of states of HH-CoKSb.

The total magnetic moment of CoKSb is $M_{\text{tot}} = 3.00$ that is consistent with the Slater-Pauling relation $M_{\text{tot}} = 18 - Z_{\text{tot}}$. The distribution of magnetic moments among the atoms on three interpenetrating fcc sublattices is $M_{\text{Co}} = 2.99$, $M_{\text{K}} = 0.02$, and $M_{\text{Sb}} = -0.01$. So it appears that HH-CoKSb has the right combination of three-sublattice ferrimagnetic order, and valence electron count $Z_{\text{tot}} = 15$ that sets the Fermi level right on the Dirac node [16]. Both $Z_{\text{tot}} = 15$ and the order of bands play significant roles in the DHS property of CoKSb as explained below. The crystal field symmetry in HH structure splits the atomic d states into doubly degenerate e_g and triply degenerate t_{2g} subspace at the Γ point. Because the electronegativity of Co and Sb are comparable, $\Delta X = 0.17$, there is a strong tendency for covalent interaction between the two. As indicated by the PDOS shown in Fig. 4, the covalent bonding mainly involves the p -states of Co and Sb near the Fermi level. The majority-spin bands are of t_{2g} -, e_g -, and p -type in the ascending order of energy, which is inverted with respect to the normal HH half-metals such as NiMnSb [32], and a conduction p -band touches the valence p -bands at the Dirac node. On the other hand, the minority-spin bands are in the normal order p -, e_g -, and t_{2g} -type, with the t_{2g} -type bands exceeding the Fermi level. Also taking to account the single s -state deep in energy, in the majority-spin direction all the nine states s through p are completely occupied. The remaining six valence electrons of $Z_{\text{tot}} = 15$ enter the minority-spin channel that is pushed up with respect to the majority-spin by the spin splitting, thus

filling the states s through p completely, while the top t_{2g} states remain completely empty. A necessary condition for DHS behavior in CoKSb is therefore that all the valence p -bands of both spins are completely occupied while all the higher bands remain completely empty so that the Fermi level comes right on the Dirac node in the majority-spin, and an open semiconductor gap appears in the minority-spin separating the valence p -type bands from t_{2g} -type conduction bands. Because all the bands through valence p are completely occupied in both spin channels, the considerations that lead to the Slater-Pauling relation $M_{\text{tot}} = 18 - Z_{\text{tot}}$ [32], remain valid. A significant feature of the majority-spin bands in CoKSb is the d - p band-inversion, while the minority-spin bands are in the normal p - d order, which is a clear indication of a topologically non-trivial electronic structure that leads to a quantum anomalous Hall state [39]. As also pointed out by Wang [18], the DHS is at the critical point of transition to a magnetic topological or Chern insulator through the application of spin-orbit coupling [40], thus resulting in a quantum anomalous Hall effect [41], which is characterized by 100% spin-polarized, massless, and dissipationless surface or edge states. Therefore, DHS materials such as CoKSb are of vital interest for ultra-fast and power-efficient spintronics of the future. The Curie temperature of DHS CoKSb is obtained to be $T_c = 730$ K, which together with thermodynamic stability and simple stoichiometric 3D structure, makes it the most viable candidate for room temperature applications so far. It must also be pointed out that the band structure of another prototype system HH-MnKSb (not shown), displays parabolic half-semimetallicity with an inverted band order similar to HH-CoKSb, but with *parabolic* p -bands (massive carriers) touching directly at the Γ point and the Fermi level. HH-MnKSb is found to have a $T_c = 870$ K. Both Dirac half-semimetals and parabolic half-semimetals are considered to be unique materials for the purpose of dissipationless spintronics [18].

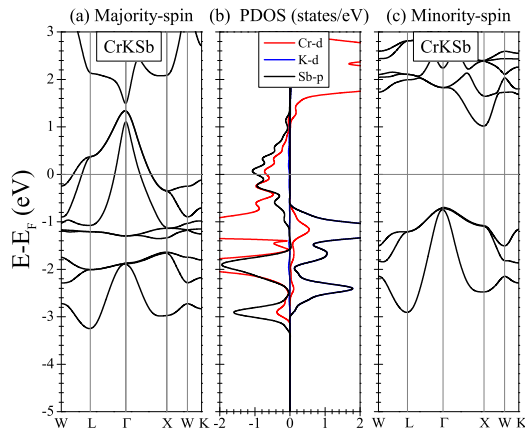


FIG. 5: Spin-resolved band structure and partial density of states of HH-CrKSb.

It is well known that zinc-blende (ZB) transition metal pnictides and chalcogenides are chemically unstable (see, also, Fig. 6) [8]. The introduction of d^0 atoms remedies this defect. Figure 5 shows the spin-resolved band structure of HH-CrKSb. The system exhibits a wide half-metallic gap $E_{\text{HM}} = 0.71$ eV, which indicates that the HM property in CrKSb is robust with respect to collapse of spin-polarization with the temperature [43, 44]. As can be noted from the PDOS in Fig. 5 (b), the HM gap arises mainly due to the spin splitting of TM atom d and sp atom p bands near the Fermi level. The total magnetic moment per formula unit is $M_{\text{tot}} = 4.00$ with the atomic distribution $M_{\text{Cr}} = 4.85$, $M_{\text{K}} = 0.02$, and $M_{\text{Sb}} = -0.87$. As in the case of ZB transition metal pnictides and chalcogenides, the corresponding Slater-Pauling relation is of the form $M_{\text{tot}} = Z_{\text{tot}} - 8$, and the HM gap results mainly from the covalent p - d hybridization directed by the local tetrahedral symmetry [32, 42]. Therefore, HH-CrKSb retains all the desirable properties of ZB-CrSb with an added bonus, i.e. chemical stability. Figure 6 shows the total energy as a function of tetragonalization parameter c/a for the HH-CrKSb and the ZB-CrSb. Whereas the ZB-CrSb shows a local maximum instability at $c/a = 1$, the HH-CrKSb has a global minimum at $c/a = 1$. In fact all the stability criteria that were checked for the other prototype systems, also are found to apply to HH-CrKSb, with a formation energy $\Delta H_f = -1.71$ eV.

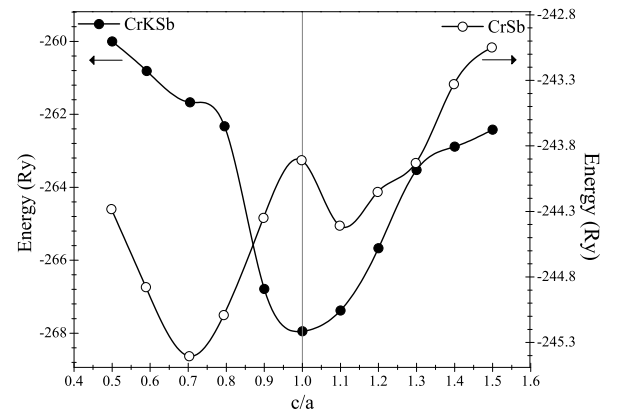


FIG. 6: Total energy is plotted against tetragonalization parameter c/a for HH-CrKSb and ZB-CrSb. The lines are guide to the eye.

To sum up, therefore, the band structure calculations reveal that chemically and magnetically stable d^0 - d HH alloys can produce all kinds of HM behavior, including Dirac half-semimetallicity that is reported for the first time in stoichiometric 3D materials. This finding opens new frontiers for massless and dissipationless spintronic applications of the future. Furthermore, the d^0 atoms are shown to stabilize the otherwise unstable chemical structure of zinc-blende transition metal pnictides and

chalcogenides without altering the p - d exchange that is mainly responsible for their half-metallicity. Because the HH structure is the thermodynamic ground state of d^0 - d ternary alloys, equilibrium preparation techniques such as arc-melting of stoichiometric quantities of constituent elements in an inert gas environment may be employed to produce bulk materials and free standing thin films. The d^0 - d HH alloys containing group II d^0 atoms, may also be better suited as electrode contacts with II-VI semi-

conductors because the bulk-like environment at the interface tends to preserve the interfacial HM property. In view of the above, a large pool of chemically and magnetically stable HH d^0 - d spintronic materials is awaiting experimental realization.

The authors wish to thank Dr. Hiroaki Ishizuka for a number of useful communications. Support from the Research Council of Shiraz University is acknowledged.

-
- [1] S. A. Wolf et al., Science **294**, 1488 (2001).
 - [2] W. E. Pickett and J. S. Moodera, Phys. Today **54**(5), 39 (2001).
 - [3] R. A. de Groot, F. M. Mueller, P. G. van Engen, and K. H. J. Buschow, Phys. Rev. Lett. **50**, 2024 (1983).
 - [4] I. Galanakis and P. H. Dederichs (Eds.), Half-metallic alloys: fundamentals and applications, Lecture notes in Physics, vol. 676 (Springer, Berlin, 2005).
 - [5] Y. Ji et al., Phys. Rev. Lett. **86**, 5585 (2001).
 - [6] W. H. Xie, Y. Q. Xu, B. G. Liu, and D. G. Pettifor, Phys. Rev. Lett. **91**, 037204 (2003).
 - [7] I. Galanakis and P. Mavropoulos, Phys. Rev. B **67**, 104417 (2003).
 - [8] Y. Liu, S. K. Bose, and J. Kudrnovsky, Phys. Rev. B **82**, 094435 (2010).
 - [9] M. Geshi, K. Kusakabe, H. Tsukamoto, and N. Suzuki, arXiv:cond-mat/0402641 (2004); K. Kusakabe, M. Geshi, H. Tsukamoto, and N. Suzuki, J. Phys.: Condens. Matter **16**, S5639 (2004).
 - [10] M. Sieberer, J. Redinger, S. Khmelevskiy, and P. Mohn, Phys. Rev. B **73** 024404 (2006).
 - [11] X. L. Wang, Phys. Rev. Lett. **100**, 156404 (2008).
 - [12] S. Ouadi, G. H. Fecher, C. Felser, and J. Kubler, Phys. Rev. Lett. **110**, 100401 (2013).
 - [13] S. Skaftouros, K. Ozdogan, E. Sasioglu, and I. Galanakis, Appl. Phys. Lett. **102**, 022402 (2013).
 - [14] L. Bainsla et al., Phys. Rev. B **91**, 104408 (2015).
 - [15] X. Wang, Z. Cheng, J. Wang, X. L. Wang, and G. Liu, J. Mater. Chem. C **4**, 7176 (2016).
 - [16] H. Ishizuka and Y. Motome, Phys. Rev. Lett. **109**, 237207 (2012).
 - [17] A. H. Castro Neto, N. M. R. Peres, K. S. Novoselov, and A. K. Geim, Rev. Mod. Phys. **81**, 109 (2009).
 - [18] X. L. Wang, Natl. Sci. Rev. **0**, 1 (2016).
 - [19] V. Pardo and W. E. Pickett, Phys. Rev. Lett. **102**, 166803 (2009).
 - [20] Z. F. Wang, Z. Liu, and F. Liu, Phys. Rev. Lett. **110**, 196801 (2013).
 - [21] X. Zhang, A. Wang, and M. Zhao, Carbon **84**, 1 (2015).
 - [22] Y. Li, D. West, H. Huang, J. Li, S. B. Zhang, and W. Duan, Phys. Rev. B **92**, 201403(R) (2015).
 - [23] T. Cai, X. Li, F. Wang, S. Ju, J. Feng, and C. D. Gong, Nano Lett. **15**, 6434 (2015).
 - [24] L. Wei, X. Zhang, and M. Zhao, Phys. Chem. Chem. Phys. **18**, 8059 (2016).
 - [25] M. Gmitra, D. Kochan, P. Hogg, and J. Fabian, Phys. Rev. B **93**, 155104 (2016).
 - [26] M. X. Chen and M. Weinert, Phys. Rev. B **94**, 035433 (2016).
 - [27] J. He, S. Ma, P. Lyu, and P. Nachtigall, J. Mater. Chem. C **4**, 2518 (2016).
 - [28] D. Xiao et al., Phys. Rev. Lett. **105**, 096404 (2010).
 - [29] S. Chadov, X. Qi, J. Kubler, G. Fecher, C. Felser, and S. C. Zhang, Nature Mater. **9**, 541 (2010).
 - [30] H. Lin et al., Nature Mater. **9**, 546 (2010).
 - [31] F. Casper, T. Graf, S. Chadov, B. Balke, and C. Felser, Semicond. Sci. Technol. **27**, 063001 (2012).
 - [32] I. Galanakis, arXiv:1302.4699 (2013); J. Surf. Interf. Mater. **2**(1), 74 (2014).
 - [33] P. Giannozzi et al., J. Phys.: Condens. Matter **21**, 395502 (2009).
 - [34] J. P. Perdew, K. Burke, and M. Ernzerhof, Phys. Rev. Lett. **77**, 3865 (1996).
 - [35] I. Galanakis, P. H. Dederichs, and N. Papanikolaou, Phys. Rev. B **66**, 134428 (2002).
 - [36] N. Sivadas, M. W. Daniels, R. H. Swendsen, S. Okamoto, and D. Xiao, Phys. Rev. B **91**, 235425 (2015).
 - [37] The same procedure is found to give $T_c = 770$ K for the well known NiMnSb, which is comparable with the corresponding experimental value of 730 K.
 - [38] L. Feng, E. K. Liu, W. X. Zhang, W. H. Wang, and G. H. Wu, J. Magn. Magn. Mater. **351**, 92 (2014).
 - [39] C. X. Liu, X. L. Qi, X. Dai, Z. Fang, and S. C. Zhang, Phys. Rev. Lett. **101**, 146802 (2008).
 - [40] C. Z. Chang et al., Science **340**, 167 (2013).
 - [41] F. D. M. Haldane, Phys. Rev. Lett. **61**, 2015 (1988).
 - [42] I. Galanakis and P. Mavropoulos, Phys. Rev. B **67**, 104417 (2003).
 - [43] A. Lezaic, P. Mavropoulos, J. Enkovaara, G. Bihlmayer, and S. Blugel, Phys. Rev. Lett. **97**, 026404 (2006).
 - [44] J. D. Aldous et al., Phys. Rev. B **85**, 060403 (2012).